Applied Physics Letters ARTICLE scitation.org/journal/apl

Acoustically driven Dirac electrons in monolayer graphene

Cite as: Appl. Phys. Lett. **116**, 103102 (2020); doi: 10.1063/1.5139498
Submitted: 20 November 2019 · Accepted: 27 February 2020 ·
Published Online: 10 March 2020

Pai Zhao,[1] Lars Tiemann,[1,a)] Hoc Khiem Trieu,[2] and Robert H. Blick[1]

AFFILIATIONS

[1]Center for Hybrid Nanostructures (CHyN), Department of Physics, Universität Hamburg, 22761 Hamburg, Germany
[2]Institute of Microsystems Technology, Hamburg University of Technology, 21703 Hamburg, Germany

[a)]Author to whom correspondence should be addressed: lars.tiemann@physik.uni-hamburg.de

ABSTRACT

We demonstrate the interaction between surface acoustic waves and Dirac electrons in monolayer graphene at low temperatures and high magnetic fields. A metallic interdigitated transducer (IDT) launches surface waves that propagate through a conventional piezoelectric GaAs substrate and couple to large-scale monolayer CVD graphene films resting on its surface. Based on the induced acousto-electric current, we characterize the frequency domains of the transducer from its first to the third harmonic. We find an oscillatory attenuation of the surface acoustic wave (SAW) velocity depending on the conductivity of the graphene layer. The acousto-electric current reveals an additional fine structure that is absent in pure magneto-transport. In addition, we find a shift between the acousto-electric longitudinal voltage and the velocity change of the SAW. We attribute this shift to the periodic strain field from the propagating SAW that slightly modifies the Dirac cone.

Probing two-dimensional electron gases (2DEGs) with acoustic sound waves is a well-established technique in condensed matter physics.[1] This technique, which is based on launching surface acoustic waves (SAWs) in the MHz- to GHz-range, is now heavily applied in optomechanics and quantum computing applications.[2–4] In a way, one can compare the interaction of electrons with an SAW to how surfers ride on a water wave. Hence, as an observer, one expects a significant variation if the energy dispersion is switched from a conventional parabolic dispersion to the quasi-relativistic linear dispersion of graphene. In other words, the surfers would be independent from the energy of the driving wave, while conventionally the velocity of sound along the surface of a medium is given by $v = \frac{\omega}{q}$, with q being the wave vector and ω the frequency of the wave.

In piezo-electric materials, the propagating sound wave is dynamically accompanied by an electrostatic potential wave that contributes to the transport of charge carriers as an acousto-electric current $I_{aec.}$.[5] The SAW amplitude attenuates exponentially into the bulk of the medium within one wavelength λ,[6] which usually exceeds the depth of conventional 2DEGs. Experiments using SAW to study GaAs/AlGaAs heterostructures have been able to detect a wave velocity shift, Δv, and attenuation, Γ, which both are functions of conductivity and reflect the conductivity oscillations in the quantum Hall regime or interactions and phase transitions.[7–9]

In the current work, we intend to probe if SAW-driven Dirac electrons at low temperatures show a different kind of response in the electro-acoustic current, as is presumed by Thalmeier[10] and others.[11] The coupling of the SAW piezoelectric field to the electron gas can attenuate the wave propagation, whereas periodic strain fields can modify the Dirac cone in graphene. Thalmeier *et al.* predict that the wave-vector dependence of the longitudinal conductivity would reveal a Dirac to Schrödinger crossover. Graphene, however, is not intrinsically piezoelectric. Hence, SAWs must be launched in a piezoelectric medium in close contact to the graphene layer in order to study acousto-electric effects. Using a (pieozoelectric) lithium niobate substrate and ZnO/SiC, it has been shown that acoustically induced currents can flow in graphene at room temperature.[12–15]

Here, we present a study of SAW in graphene in the $qd \ll 1$ regime at 4.2 Kelvin and under perpendicular magnetic fields, where d is the thickness of monolayer graphene. We chose a gallium arsenide (GaAs) semiconductor as the piezoelectric medium due to its versatile applicability in high electron mobility heterostructures or integrated high frequency circuits. We calculate changes in the SAW velocity based on magneto-transport measurements obtained in a standard setup using a constant ac current. Our sample processing begins with electron beam lithography to define interdigitated transducers (IDTs) on top of a piezoelectric insulating GaAs substrate that launches SAWs. In a wet-transfer process,[16] monolayer CVD graphene is placed

on the substrate. At a distance of 200 μm and in the propagation path of the SAWs, a Hall bar of 1 mm × 0.25 mm is fabricated by optical lithography. Deposition of Au/Ti is used for both the IDTs and Ohmic contacts to the Hall bar. The IDT pitch corresponds to acoustic wavelengths of 8 μm for the fundamental, 4 μm for the second, and 2.6 μm for the third harmonic. Prior to our measurements, the sample was thermally annealed in vacuum at 100° C for 48 h to reduce the amount of contaminants on the graphene surface. The sample configuration and the overall setup are schematically shown in Fig. 1. The right-hand panels show a scanning electron microscopic image and a Raman spectrum of the graphene layer, indicating that we are indeed working on monolayer graphene.

Transport measurements are performed with SR830 lock-in amplifiers to detect currents and voltages. They also provide a reference to the signal generator for amplitude modulation (AM) of the radio frequency (RF) signal applied to the IDT.[17,18] In the current setup, we work with one IDT firing at the graphene sample. All measurements are performed at 4.2 K. Graphene is characterized by standard magneto-transport using an ac current of $I_{ac} \approx 2$ nA (red branch connected to C4 in Fig. 1). Figure 2 shows the resulting longitudinal resistance, R_{xx}, and Hall-resistance, R_{xy}, as a function of the magnetic field, $\vec{B}$, at a back-gate voltage of $V_g = 0$ V. The formation of a plateau in R_{xy} for $|B| > 6$ T signals Landau quantization. From the Hall resistance, we can deduce the intrinsic electron density[19] of $n = 7.9 \times 10^{11}$ cm^{-2} and the mobility of $\mu = 4.15 \times 10^{2}$ cm^2 V^{-1} s^{-1}. The chip carrier back contact acts as an electrode for tuning the carrier density. The small capacitance of the substrate, however, limits the tunability of the carrier concentration to approximately 3% (inset Fig. 2). Thus, all subsequent measurements are performed at $V_g = 0$ V. For this density, the carriers in graphene reside in the low energy, linear branch of the dispersion relation where electrons do not behave classically but follow Dirac physics.

For tracing the SAW response, we disconnect the ac source and ground contact C4 (light blue branch in Fig. 1). This is necessary in order to close the electrical circuit and enable a steady acousto-electric current. The SAW is launched by applying an AM RF power to the

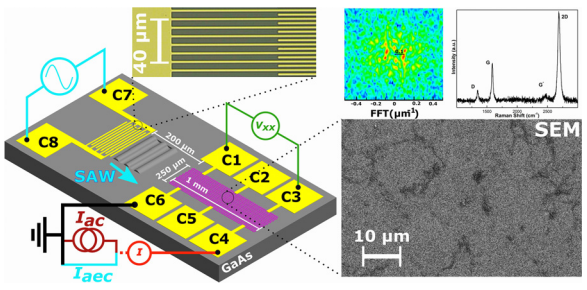

FIG. 1. Sample design and sketch of the measurement setup: an IDT (top inset) with contacts C7 and C8 was fabricated on a GaAs semi-insulating piezoelectric substrate (gray). By applying an RF signal, an SAW (light blue) is launched that propagates through the graphene-Hallbar of 1 mm length (magenta honeycomb lattice). The right-hand lower panel shows an SEM image that highlights defects and boundaries existing in our CVD-graphene. The upper center panel is an FFT analysis of the SEM image [blue represents minima and red maxima], which will be discussed later in the main text. The ratio of the G and 2D peaks in the Raman spectrum shown on the right-hand upper panel demonstrates the existence of a single layer of graphene. A magnetic field is applied perpendicular to the sample (not shown).

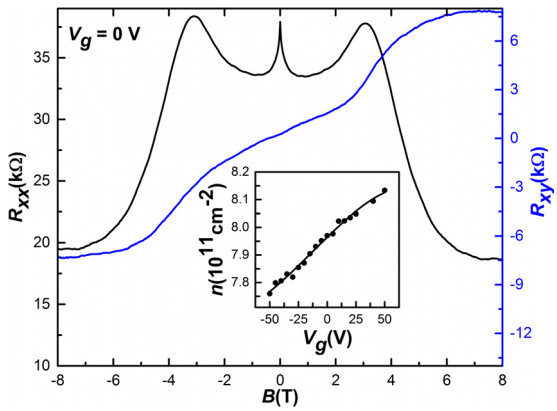

FIG. 2. Longitudinal resistance (black solid line) and Hall resistance (blue solid line) measured by passing a constant ac current through the graphene Hall bar at 4.2 K and $V_g = 0$ V. Landau quantization is signaled by a Hall plateau for $|B| > 6$ T. Inset: carrier density as a function of back gate voltage.

IDT. From the measurement of the acousto-electric current as a function of frequency (shown in Fig. 3), we identify the (fundamental) first harmonic at 571.5 MHz,[20] the second harmonic at 1.175 GHz, and the third harmonic at 1.684 GHz. For the first harmonic, I_{aec} exhibits a linear dependence on the applied RF power.[14,15,21] Acousto-electric magneto-transport can therefore be performed with the same current amplitude of $I_{ac} \approx I_{aec} \approx 2$ nA at 0 T as in the previous magneto-transport experiments using an ac signal.

The oscillating electrostatic potential that accompanies the propagation of an SAW in a piezoelectric medium depends on the screening capabilities of mobile carriers. The SAW velocity is thus a function of the conductivity and can be expressed as

$$\frac{\Delta v}{v} = \frac{K_{\text{eff}}^2}{2} \cdot \frac{1}{1 + (\sigma_{xx}/\sigma_M)^2}, \tag{1}$$

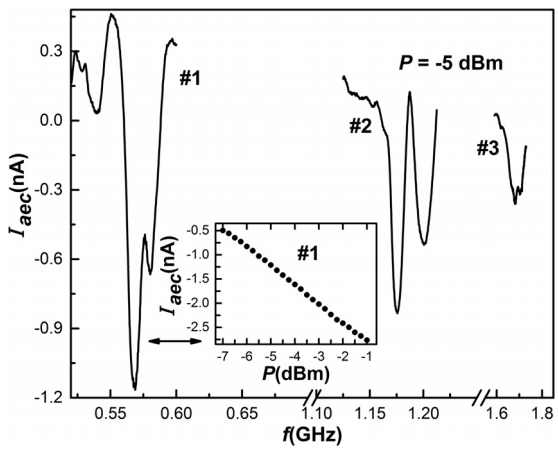

FIG. 3. Acousto-electric current as a function of frequency at −5 dBm with the first harmonic resonance (#1) at 571.5 MHz, the second harmonic resonance (#2) at 1.175 GHz, and the third harmonic resonance (#3) at 1.684 GHz. Inset: linear power-dependence of the acousto-electric current for the first harmonic resonance of the IDT.

with

$$\sigma_M = \nu\varepsilon_0(1+\varepsilon_G), \tag{2}$$

$$\sigma_{xx} = \frac{\rho_{xx}}{\rho_{xx}^2+\rho_{xy}^2}, \tag{3}$$

$K_{\text{eff}}^2 = 0.06\%$ is the piezoelectric coupling coefficient for GaAs, which we use as the piezoelectric substrate, and ϵ_G is the dielectric constant of graphene.[22] The longitudinal resistivity, ρ_{xx}, and Hall resistivity, ρ_{xy}, are obtained from magneto-transport in the standard ac signal, as shown in Fig. 2.

In our sample, interfacial van der Waals bonds work as a bridge between the monolayer graphene and the GaAs surface, which will also determine the coupling of the SAWs to the graphene. To our knowledge, no reports exist on the exact value of the van der Waals force between graphene and GaAs. However, for graphene on SiO_2, both density functional theory and experimental methods[23–26] yield adhesion energies at the interface of the order of ∼100 mJ/m^2 or van der Waals forces of the order of ∼100 MPa, respectively. Here, we assume similar orders of magnitude for the GaAs interface.

Graphene is known to exhibit rippling with a periodicity of a few nanometers when it conforms to an underlying substrate.[27] This would give rise to local decoupling from the substrate. However, as the SAW wavelength exceeds this rippling by several orders of magnitude and in light of strong van der Waals forces, we assume that Eq. (1) remains valid in our case. Figure 4(a) shows the SAW velocity change calculated from the conductivity determined by standard magneto transport following Eq. (1). With decreasing conductivity, $\frac{\Delta v}{v}$ increases until a maximum is reached. This behavior was also observed in conventional 2DEGs in GaAs heterostructures and confirms the applicability to our graphene system and the values of the effective piezoelectric coupling, K_{eff}^2, and characteristic conductivity, σ_M. Hence, it already appears likely that the charge carriers behave similar to conventional 2DEGs in semiconductors.

Figure 4(b) shows the longitudinal voltage drop generated by the acousto-electric current. We find that the pronounced maxima in the longitudinal voltage are shifted with respect to maxima in the velocity change.[1] We also observe an oscillatory fine structure in the acousto-electric longitudinal voltage drop over the entire magnetic field range, which does not appear in the conventional magneto-transport using a constant ac signal. Furthermore, we observe similar features at other harmonics. This fine structure also appears at the other IDT's harmonics, as shown in Fig. 4(c).

While the fine structure is reminiscent of commensurability oscillations[28] that appear when the cyclotron orbits match periodic background potentials, the magnetic length, $l_B = \sqrt{\hbar/eB}$, at 10 mT is already much smaller than the SAW wavelength. Thus, it is impossible to reconcile the field dependence of the cyclotron orbits with our data. We assume that the fine structure is an interference effect related to the disordered nature of our sample.

As shown by the SEM image in Fig. 1, the CVD graphene appears to have ripples and wiggles. An FFT analysis of the graphene's SEM images reveals dominant structures in real space with 1 μm and 10 μm in size (upper central panel of Fig. 1). These structural dimensions are in agreement with previous reports[29,30] on CVD graphene and match the length scale of the acoustic wave. The geometric commensurability between the wavelength and defect sizes and the appearance of the fine structure is unlikely to be coincidental. The interaction between the acoustic wave and defects in our CVD graphene appears to depend on the wavelength, as previously reported.[21]

We propose that defects such as grain boundaries, wiggles, and ripples locally alter the conductivity, either by strain and the resulting

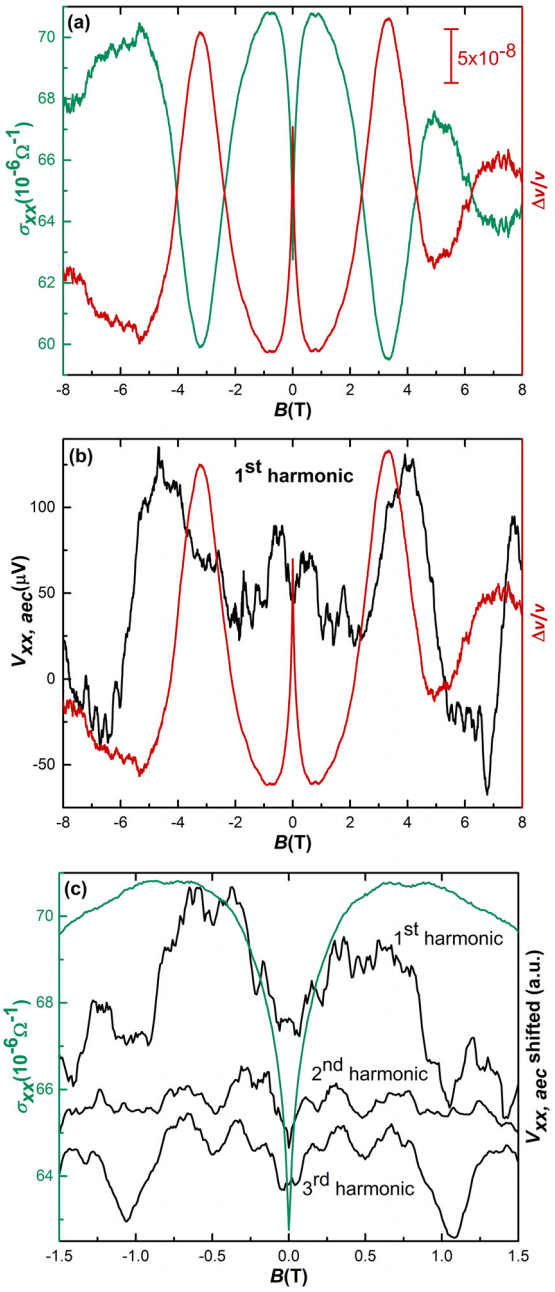

FIG. 4. (a) SAW velocity change (right-hand axis) calculated from the conductivity (left-hand axis) measured by the standard magneto-transport shown in Fig. 2. (b) Longitudinal voltage oscillations (left-hand axis) generated by the acousto-electric current at the first harmonic and oscillations of SAW velocity (right-hand axis) as calculated in sub figure (a). (c) Longitudinal voltage induced by the acousto-electric current at the IDT's first to third harmonic (see the text for further details). The curves were shifted for clarity.

changes in the band structure, by locally varying doping or by a broken lattice that induces edges. An SAW passing through the area covered by the graphene will thus experience a non-uniform attenuation and may branch off into a multitude of secondary waves. The carriers propagating in the potentials of secondary waves can pick up geometrical phases. The integral over all paths and acquired phase differences returns corrections to the voltage drop that also depends on the magnetic field; this is comparable to universal conductance fluctuations, which originate from the interference between the trajectories of all electronic paths in strongly disordered materials.[31,32]

Figure 4(c) compares the acousto-electric voltage to the conductivity in the low magnetic field regime. Here, the overall conductivity of the graphene is high, resulting in a strong interaction between SAW and electrons. Surface acoustic waves of the second harmonics interact differently with the defects than the other harmonics, and the absence of a pronounced fine structure in the acousto-electric voltage signals that the interference corrections are small. The third harmonic shows a pronounced minimum at $\pm$ 1 T. Here, the acquired phase differences by the electrons return a large negative correction to the acousto-electric voltage, which then exhibits a minimum.

The shift between the calculated velocity change and the measured acousto-electric voltage as shown in Fig. 4(b), on the other hand, seems to be indicative of corrugation strain induced by the dynamically propagating SAW. The shear force generated by the SAW propagation is of the order of $\sim$0.1 MPa for graphene on polymer substrates.[33] The shear strength of graphene on GaAs is potentially bigger since the van der Waals force of graphene on GaAs is larger than on polymer.[26] Shear strain in graphene is predicted to induce strong gauge fields and would also affect the Landau quantization.[34,35] Therefore, strain is a strong candidate to explain the shift between the calculated velocity change and the measured acousto-electric voltage, as shown in Fig. 4(b).

In summary, we presented a technology to study the carrier dynamics of Dirac electrons in graphene at high magnetic fields and low temperature using acousto-electric currents. We demonstrated the coupling between the propagating SAW and the electronic system through the attenuation of the SAW depending on the conductivity of graphene. We can state that the electrons in this Dirac material behave mostly classical. This is in agreement with the reports of SAW in graphene on lithium niobate substrates at room temperature.[14] However, it appears that there exists a fine structure, which cannot be explained with a classical electron dispersion. This method is easily transferable to other van der Waals materials and other piezoelectric substrates even at room temperature.

We acknowledge support from the Partnership for Innovation, Education, and Research (PIER). We also thank the Excellence Cluster Center for Ultrafast Imaging (CUI) of the Deutsche Forschungsgemeinschaft (DFG) for support under Contract No. EXC-1074. In particular, we would like to thank Steve H. Simon and Lev G. Mourokh for fruitful discussions.

REFERENCES

[1]S. H. Simon, Phys. Rev. B **54**, 13878–13884 (1996).
[2]J. Koch, T. M. Yu, J. Gambetta, A. A. Houck, D. I. Schuster, J. Majer, A. Blais, M. H. Devoret, S. M. Girvin, and R. J. Schoelkopf, Phys. Rev. A **76**, 042319 (2007).
[3]M. V. Gustafsson, T. Aref, A. F. Kockum, M. K. Ekström, G. Johansson, and P. Delsing, Science **346**, 207–211 (2014).
[4]P. Delsing, A. N. Cleland, M. J. A. Schuetz, J. Knörzer, G. Giedke, J. I. Cirac, K. Srinivasan, M. Wu, K. C. Balram, C. Bäuerle, T. Meunier, C. J. B. Ford, P. V. Santos, E. Cerda-Méndez, H. Wang, H. J. Krenner, E. D. S. Nysten, M. Weiß, G. R. Nash, L. Thevenard, C. Gourdon, P. Rovillain, M. Marangolo, J.-Y. Duquesne, G. Fischerauer, W. Ruile, A. Reiner, B. Paschke, D. Denysenko, D. Volkmer, A. Wixforth, H. Bruus, M. Wiklund, J. Reboud, J. M. Cooper, Y. Fu, M. S. Brugger, F. Rehfeldt, and C. Westerhausen, J. Phys. D: Appl. Phys. **52**, 353001 (2019).
[5]J. M. Shilton, D. R. Mace, V. I. Talyanskii, M. Y. Simmons, M. Pepper, A. C. Churchill, and D. A. Ritchie, J. Phys: Condens. Matter **7**, 7675 (1995).
[6]G. Farnell, *Types and Properties of Surface Waves, in Topics in Applied Physics: Acoustic Surface Waves* (Springer-Verlag Berlin Heidelberg, 1978).
[7]A. Wixforth, J. P. Kotthaus, and G. Weimann, Phys. Rev. Lett. **56**, 2104–2106 (1986).
[8]A. Wixforth, J. Scriba, M. Wassermeier, J. P. Kotthaus, G. Weimann, and W. Schlapp, Phys. Rev. B **40**, 7874–7887 (1989).
[9]R. L. Willett, M. A. Paalanen, R. R. Ruel, K. W. West, L. N. Pfeiffer, and D. J. Bishop, Phys. Rev. Lett. **65**, 112–115 (1990).
[10]P. Thalmeier, B. Dóra, and K. Ziegler, Phys. Rev. B **81**, 041409 (2010).
[11]A. Hernandez-Minguez, Y.-T. Liou, and P. V. Santos, J. Phys. D: Appl. Phys. **51**, 383001 (2018).
[12]V. Miseikis, J. E. Cunningham, K. Saeed, R. O'Rorke, and A. G. Davies, Appl. Phys. Lett. **100**, 133105 (2012).
[13]P. V. Santos, T. Schumann, M. H. Oliveira, J. M. J. Lopes, and H. Riechert, Appl. Phys. Lett. **102**, 221907 (2013).
[14]L. Bandhu, L. M. Lawton, and G. R. Nash, Appl. Phys. Lett. **103**, 133101 (2013).
[15]L. Bandhu and G. R. Nash, Nano Res. **9**, 685–691 (2016).
[16]T. J. Lyon, J. Sichau, A. Dorn, A. Zurutuza, A. Pesquera, A. Centeno, and R. H. Blick, Appl. Phys. Lett. **110**, 113502 (2017).
[17]B. Lüthi, *Physical Acoustics in the Solid State* (Springer-Verlag Berlin Heidelberg, 2005).
[18]J. Heil, I. Kouroudis, and P. Thalmeier, J. Phys. C: Solid State Phys. **17**, 2433 (1984).
[19]The intrinsic carrier type and concentration are subject to the details of the sample preparation and surface doping. For CVD graphene on SiO_2, the intrinsic density is smaller by a factor of at least 2, while the carrier mobility is higher. The different surface chemistry of GaAs and the resulting different number/types of trapped adsorbents between graphene and GaAs surface determine carrier concentration and mobility.
[20]A resonance of 571 MHz for a wavelength of 8 μm corresponds to a sound velocity of about 4500 m/s. This is about 1.5 times larger than reported for ideal SAWs in GaAs. Such an enhancement of the SAW velocity by 50% has been reported for acoustic waves which also have considerable bulk components, [see e.g., Ruppel and Fjeldly, *Advances in Surface Acoustic Wave Technology, Systems and Applications* (World Scientific, 2001); J. Appl. Phys. **58**, R1 (1985); J. Appl. Phys. **79**, 8936 (1996)].
[21]L. Bandhu and G. R. Nash, Appl. Phys. Lett. **105**, 263106 (2014).
[22]D. C. Elias, R. V. Gorbachev, A. S. Mayorov, S. V. Morozov, A. A. Zhukov, P. Blake, L. A. Ponomarenko, I. V. Grigorieva, K. S. Novoselov, and A. K. Geim, Nat. Phys. **7**, 701 (2011).
[23]Z. H. Aitken and R. Huang, J. Appl. Phys. **107**, 123531 (2010).
[24]S. P. Koenig, N. G. Boddeti, M. L. Dunn, and J. S. Bunch, Nat. Nanotechnol. **6**, 543 (2011).
[25]W. Gao, P. Xiao, G. Henkelman, K. M. Liechti, and R. Huang, J. Phys. D: Appl. Phys. **47**, 255301 (2014).
[26]D. Akinwande, C. J. Brennan, J. S. Bunch, P. Egberts, J. R. Felts, H. Gao, R. Huang, J.-S. Kim, T. Li, Y. Li, K. M. Liechti, N. Lu, H. S. Park, E. J. Reed, P. Wang, B. I. Yakobson, T. Zhang, Y.-W. Zhang, Y. Zhou, and Y. Zhu, Extreme Mech. Lett. **13**, 42–77 (2017).
[27]A. Fasolino, J. H. Los, and M. I. Katsnelson, Nat. Mater. **6**, 858 (2007).
[28]D. Weiss, K. v Klitzing, K. Ploog, and G. Weimann, Europhys. Lett. **8**, 179 (1989).

[29]X. Li, W. Cai, J. An, S. Kim, J. Nah, D. Yang, R. Piner, A. Velamakanni, I. Jung, E. Tutuc, S. K. Banerjee, L. Colombo, and R. S. Ruoff, Science **324**, 1312–1314 (2009).
[30]C. Mattevi, H. Kima, and M. Chhowalla, J. Mater. Chem. **21**, 3324 (2011).
[31]C. P. Umbach, S. Washburn, R. B. Laibowitz, and R. A. Webb, Phys. Rev. B **30**, 4048 (1984).
[32]P. A. Lee and A. D. Stone, Phys. Rev. Lett. **55**, 1622 (1985).
[33]T. Jiang, R. Huang, and Y. Zhu, Adv. Funct. Mater. **24**, 396–402 (2014).
[34]K.-I. Sasaki, Y. Kawazoe, and R. Saito, Prog. Theor. Phys. **113**, 463–480 (2005).
[35]F. Guinea, M. I. Katsnelson, and A. K. Geim, Nat. Phys. **6**, 30 (2010).